Technical Note **KI 03 08 0373 R**

THE RAPID GROWTH PHASE IN MICE IS ASSOCIATED WITH INCREASING SUSCEPTIBILITY TO ACUTE RENAL FAILURE

Richard A. Zager, MD [1, 2]

Ali CM Johnson, BS [2]

Masayo Naito, MD, PhD [2]

Steve Lund, BS [2]

Nayeon Kim, BS [2]

Karol Bomsztyk, MD [1]

From: the Department of Medicine, University of Washington (1), and the Fred Hutchinson Cancer Research Center (2), Seattle, WA 98109

Address correspondence to:

Richard A. Zager, MD
Fred Hutchinson Cancer Research Center
1100 Fairview Ave. N; Room D2-190
Seattle, WA 98109
Email: dzager@fhcrc.org
Tele: (206) 667-6222
FAX: (206) 667-6519

This work was supported by research grants from the National Institutes of Health [DK-R37-38431; DK- 68520 (RZ); DK-R37-45978 and GM45134 (KB)].

Word counts: Abstract, 249; manuscript, 1453; Concise Methods, 475.

ABSTRACT

In recent years, experimental studies of acute renal failure (ARF) have been most widely conducted in young mice that are in a rapid growth phase. However, the impact of early growth and development on renal susceptibility to ARF has not been defined. The present study has begun to address this issue by testing the severity of endotoxemic-, glycerol-, and maleate-induced ARF in male CD-1 mice ranging from 3-16 weeks of age (17-45 gm). The potential for age to alter the expression of at least one injury modifier, cellular cholesterol, was also assessed. The severity of each ARF model (BUN / histology) directly correlated with mouse wt. and age ($p < 0.001$). Progressive age- dependent reductions in renal cholesterol content were also observed. The latter were paralleled by stepwise decrements in mRNA levels of two key cholesterol homeostatic genes (HMG CoA reductase, HMGCR, and low density lipoprotein receptor, LDL-R). The mRNA reductions were paralleled by falling RNA polymerase II and transcription factor (SREBP 1 / 2) densities at the HMGCR and LDL-R genes. Hence, we conclude that: 1) the early phase of mouse growth can profoundly alter renal susceptibility to diverse forms of ARF; 2) these changes can reflect fundamental fluxes in select, and likely protean, biochemical and molecular changes at the whole tissue and genomic levels (cholesterol being one such example); 3) ChIP is a powerful tool for studying such changes; and 4) the early growth period needs to be carefully controlled for when conducting studies of experimental ARF.

INTRODUCTION

Mice have become the most widely used animal species for studies of experimental acute renal failure (ARF). This is due to their relatively low cost, the great variety of strains ± genetic modifications that are available, and the wide range of molecular probes (e.g., monoclonal antibodies) that permit study of specific injury pathways. Relatively young mice (2-4 months of age) are most commonly used, presumably because short periods of vivarium housing mitigate time constraints and expense.

During the first 4 months of age, mice undergo rapid growth and development. For example, widely used CD-1 mice approximately triple their body weight from 3 to 16 weeks of age. It has previously been demonstrated that as rodents advance from adulthood into old age (e.g., from ~6 months to ~2 years), increasing susceptibility to ischemic ARF results (1-6). This may arise from a progressive loss of renal functional reserve, and possible aging- induced renal biochemical changes. In contrast, the potential impact of the *early* growth period (e.g., the first 1-4 months of life) on renal susceptibility to injury has not been well defined. Hence, this study was conducted as an initial exploration of this issue.

RESULTS and DISCUSSION

Between 3 and 16 weeks of age, the employed CD-1 mice manifested rapid growth, with an approximate tripling of body wt (Fig. 1, left). This is consistent with data from the animal supplier (Charles River Laboratories). A proportionate increase in kidney mass was observed, as denoted by a near constant relationship between single kidney vs. total body wt (~0.65%; Fig. 1, right). To test whether susceptibility to ARF is altered during this time frame, the mice were categorized as being 'juvenile' (age 3-4 weeks), 'adolescent' (5-6 weeks), or 'mature' (10-16 weeks) and challenged with either intravenous endotoxin (lipopolysaccharide, LPS; ref.7), intramuscular glycerol (8-10), or intraperitoneal maleate (11-13) injection. These three ARF models were chosen for study because they induce renal injury by highly divergent mechanisms. Endotoxemia causes a predominantly hemodynamic form of ARF (7, 14,15), as evidenced by

renal vasoconstriction, but maintenance of essentially normal renal histology (e.g., ref. 7). As shown in Fig. 2, left, the severity of LPS- induced ARF directly correlated with animal age / wt, as assessed either by relative degrees of azotemia for the three age groups ($p<0.001$), or by the overall correlation coefficients between individual mouse wts vs. BUN concentrations. In contrast to LPS, glycerol evokes a structural form of ARF, as denoted by proximal tubule necrosis and heme protein cast formation (8-10). This results from glycerol- induced rhabdomyolysis and hemolysis, with subsequent heme iron driven proximal tubule oxidative stress (8-10). Again, a striking correlation between age / body wt and the severity of ARF was observed, whether injury severity was assessed functionally (BUN: Fig. 2) or by renal histology (Fig. 3). In contrast to glycerol and LPS which induce both extra-renal and renal injury, maleate toxicity is specific for the proximal tubule (12,13,16). This is due to selective maleate transport / uptake by this nephron segment (11, 16). With subsequent intracellular metabolism (13), toxic intermediaries result, producing mitochondrial dysfunction and a profound ATP depletion state. This culminates in a form of injury that recapitulates most critical features of post- ischemic ARF (12). Using this maleate model, a striking direct relationship between animal wt / age and the severity of ARF again was observed, as gauged by BUNs (Fig. 2) and renal histology (Fig. 3). It is notable that the greatest variation in renal injury with each of the three ARF models was found in the 'adolescent' age group (e.g., BUN coefficients of variation as high as 65%). This implies that it is during this intermediate time frame that the most profound transition from an 'injury resistant' to an 'injury sensitive' phenotype occurs. Finally, it is notable that increasing either the maleate or glycerol dosages in 'juvenile' mice failed to induce the same degree of injury that was observed in 'mature' mice with lesser toxin doses (Fig. 4). This underscores the relative degree of protection that the youngest mice express. Finally, although this study employed male CD-1 mice, we have observed comparable degrees of protection in young female mice, and this correlates with body weight. Thus, the above described results do not appear to be gender specific.

The explanation for the profound impact of rapid mouse growth / development on ARF susceptibility remains unknown, but it undoubtedly represents a fertile avenue for future study. It is almost certainly multi-factorial in nature, and may well operate via different pathways in different ARF models. In an attempt to demonstrate that the rapid growth phase can, in fact, alter the expression of specific injury- modifying molecules, we sought age dependent differences in the expression renal cholesterol, a previously well documented renal cytoprotectant (17-20). In the aftermath of acute tubular injury, cellular cholesterol levels rise. This stabilizes the plasma membrane, and hence, prevents plasma membrane rupture during superimposed toxic or ischemic stress (17-20). Therefore, we questioned whether the highest renal cholesterol levels might be observed in the youngest mice, with progressive age- related reductions thereafter. Indeed, as shown in Fig. 5, left, this was the case. Renal tubular cholesterol content primarily reflects de novo HMG CoA reductase (HMGCR)- driven synthesis, and low density lipoprotein- receptor (LDL-R)- mediated cholesterol extraction from plasma (17-20). To assess whether, or which, of these pathways might be operative, we measured HMGCR mRNA and LDL-R mRNA levels during the studied growth period. As shown in Fig. 6, both HMGCR and LDL-R mRNAs progressively decreased with advancing age, paralleling the reductions in cholesterol content. This suggests that both synthetic and uptake pathways may contribute to the observed, age dependent, differences in renal cholesterol content. Of note, serum cholesterol progressively *increased* with age despite *falling* renal cholesterol levels (Fig. 5, right). While by no means conclusive, this reciprocal relationship between renal and serum cholesterol levels would be consistent with increased LDL-R mediated cholesterol extraction from blood, and hence, rising renal cholesterol levels.

To test whether the above noted changes in HMGCR mRNA and LDL-R mRNA levels reflected differences in gene transcription, rather than simply a potential difference in mRNA stabilities, we measured RNA polymerase II (Pol II) densities at the start and end exons of the HMGCR and LDL-R genes by microplate-based matrix chromatin immunoprecipitation (ChIP)

technology (see Methods). Of note, Pol II density is both a mediator of, and a surrogate marker for, rates of gene transcription (21-23). Indeed, at both start and end HMGCR and LDL-R gene exons, Pol II expression decreased with advancing age, thereby paralleling the observed mRNA and cholesterol declines (Fig. 7). To further assess whether age dependent differences in renal cholesterol content are reflected by differences in gene regulation, densities of Pol II, SREBP-1, and SREBP-2 (Sterol Regulatory Element Binding Protein transcription factors 1, 2; ref. 24, 25) at two sites within the HMGCR promoter were assessed. Again consistent with the mRNA data, the youngest mice had the highest amounts of Pol II, SREBP-1, and SREBP-2 at the HMGCR promoter (Fig. 8). That Pol II and SREBP densities at silent genes (rDNA, β globin) did not vary according to age (Fig. 9) indicates the specificity of the above noted Pol II / SREBP results. Thus, the entire assessed HMGCR cholesterol synthetic axis (from ↑ transcription factors at the promoter → ↑ Pol II at the promoter → ↑ Pol II along the gene → ↑ mRNA → ↑ cholesterol) was relatively over-expressed in the 'juvenile' vs. the 'mature' animals. Of even broader significance than these specific findings, the Pol II and SREBP data underscore the great potential utility of matrix ChIP assay for studying in vivo genomic, and potentially, epigenomic events in in vivo renal tissue.

Finally, we wish to underscore that we *do not conclude that the cholesterol pathway is responsible for the age dependent differences in ARF susceptibility noted in this study*. Rather, the age dependent changes within the cholesterol axis simply *illustrate* the dynamic nature of cellular processes that are in flux during early growth and development. Undoubtedly, changing levels of many other injury modifiers, such as growth factors (e.g., EGF, IGF, HGF), cell cycle regulatory proteins (e.g., p21), and potent cytoprotective molecules (e.g., heme oxygenase -1) could also be in flux during 1-4 months of age. In light of these theoretical considerations, and the results of the present study, it would appear that great attention needs to be paid to mouse

age when conducting studies of this type. Finally, the present study indicates that matrix ChIP assay is a powerful new tool that can be applied to the study of such issues.

CONCISE METHODS

ARF protocols: All experiments were conducted with male CD-1 mice (Charles River Laboratories, Wilmington, MA) that were obtained at either 2-3 weeks (wt ~17 gms) or 4-5 weeks (wt ~25 gms) of age. They were maintained under routine vivarium conditions with free food and water access. They were arbitrarily assigned to one of three age groups: 'Juvenile', 3-4 weeks, ~ 20 gms; 'Adolescent', 5-6 weeks, ~30 gm; or 'Mature', 10-16 weeks, ~40 gms). The 'mature' group consisted of mice that were obtained at either at 2-3 weeks or 4-5 weeks of age and allowed to mature in this institution's vivarium. Because the age and weight of the mice represented a continuum within and between groups (rather than fixed arbitrary values), the results from the ARF experiments were compared both between the arbitrary groups and as overall correlations between age / weight vs. the severity of ARF (as gauged by BUN concentrations). The following three ARF models were employed: 1) an E. coli endotoxemic model of ARF (2 mg/Kg via tail vein injection; ref. 7); Na maleate nephrotoxicity (600 mg/Kg IP; ref. 12); and 3) glycerol- induced ARF (50% solution; 9 mL/Kg, administered in a divided IM dose in each hind limb; ref. 10). Approximately 18-20 hrs post injections, the mice were anesthetized with pentobarbital (40-50 mg/Kg; IP), a serum sample was obtained from the vena cava for BUN analysis, and the kidneys were resected and prepared for ChIP and mRNA analyses. Kidneys from the 'juvenile' and 'mature' mouse groups that underwent the maleate or glycerol challenges were cut longitudinally, fixed in 10% buffered formalin, 4 micron sections were cut and stained (H&E), and examined by light microscopy to evaluate the extent of injury (tubular necrosis, cast formation).

Baseline renal assessments: The following baseline parameters for the mice in different age groups were assessed: 1) single kidney weight (given as % total body wt); 2) BUN concentrations; 3) renal cortical mRNAs for HMGCR and LDL-R (RT-PCR; ref. 20, 26-28); 4)

renal cortical cholesterol content (gas chromatography; ref. 26); 5) RNA polymerase II (Pol II) density at the start and end exons of the HMGCR and LDL-R gene (tissues prepared as per ref. 29, and assayed by microplate-based matrix ChIP assay (30)]; 6) Pol II density at the HMGCR promoter (-100 and -400 bp; 5' to TSS); 7) SREBP-1 and SREBP- 2 (transcription factors) at the HMGCR promoter (-100 bp); and 8) 'negative controls': Pol II at 18S ribosomal DNA (rDNA; ref. 30); SREBP-1 and SREBP-2 at a "silent" kidney gene (β globin). ChIP DNA data were expressed as a fraction of input DNA (30). All values are given as means ± 1 SEM. Statistical analyses were performed either by unpaired Student's t testing for analyzing two sets of data, by ANOVA if multiple groups were compared (after testing by Student's t test with Bonferroni correction), and by calculating correlation coefficients.

Financial Disclosure: None to report

REFERENCES

1. Miura K, Goldstein RS, Morgan DG, Pasino DA, Hewitt WR, Hook JB: Age-related differences in susceptibility to renal ischemia in rats. Toxicol Appl Pharmacol 87:284-296, 1987

2. Zager RA, Alpers CE: Effects of aging on expression of ischemic acute renal failure in rats. Lab Invest 61: 290-294, 1989

3. Sabbatini M, Pisani A, Uccello F, Serio V, Serù R, Paternò R, Cianciaruso B, Fuiano G, Andreucci M: Atorvastatin improves the course of ischemic acute renal failure in aging rats. J Am Soc Nephrol 15:901-909, 2004

4. Qiao X, Chen X, Wu D, Ding R, Wang J, Hong Q, Shi S, Li J, Xie Y, Lu Y, Wang Z: Mitochondrial pathway is responsible for aging-related increase of tubular cell apoptosis in renal ischemia/reperfusion injury. J Gerontol A Biol Sci Med Sci 60: 830-9, 2005

5. Chen G, Bridenbaugh EA, Akintola AD, Catania JM, Vaidya VS, Bonventre JV, Dearman AC, Sampson HW, Zawieja DC, Burghardt RC, Parrish AR: Increased susceptibility of aging kidney to ischemic injury: identification of candidate genes changed during aging, but corrected by caloric restriction. Am J Physiol 293: F1272-1281, 2007

6. Miyaji T, Hu X, Yuen PS, Muramatsu Y, Iyer S, Hewitt SM, Star RA: Ethyl pyruvate decreases sepsis-induced acute renal failure and multiple organ damage in aged mice. Kidney Int 64:1620-1631, 2003.

7. Zager RA, Johnson AC, Lund S, Hanson SY, Abrass CK. Levosimendan protects against experimental endotoxemic acute renal failure. Am J Physiol 290: F1453-1462, 2006

8. Nath KA, Balla G, Vercellotti GM, Balla J, Jacob HS, Levitt MD, Rosenberg ME: Induction of

heme oxygenase is a rapid, protective response in rhabdomyolysis in the rat. J Clin Invest 90: 267-270, 1992

9. Tracz MJ, Juncos JP, Grande JP, Croatt AJ, Ackerman AW, Rajagopalan G, Knutson KL, Badley AD, Griffin MD, Alam J, Nath KA: Renal hemodynamic, inflammatory, and apoptotic responses to lipopolysaccharide in HO-1-/- mice. Am J Pathol 170:1820-1830, 2007

10. Zager RA: Combined mannitol and deferoxamine therapy for myohemoglobinuric renal injury and oxidant tubular stress. Mechanistic and therapeutic implications. J Clin Invest 90:711-719, 1992

11. Kellerman PS: Exogenous adenosine triphosphate (ATP) preserves proximal tubule microfilament structure and function in vivo in a maleic acid model of ATP depletion. J Clin Invest 92: 1940-1949, 1993

12. Zager RA, Johnson AC, Naito M, Bomsztyk K: Maleate nephrotoxicity: mechanisms of injury and correlates with ischemic/hypoxic tubular cell death. Am J Physiol 294:F187-197, 2008

13. Pacanis A, Strzelecki T, Rogliski J: Effects of maleate on the content of CoA and its derivatives in rat kidney mitochondria. J Biol Chem 256: 13035-13038, 1981

14. Wang W, Zolty E, Falk S, Summer S, Zhou Z, Gengaro P, Faubel S, Alp N, Channon K, Schrier R: Endotoxemia-related acute kidney injury in transgenic mice with endothelial overexpression of GTP cyclohydrolase-1. Am J Physiol 294: F571-576, 2008

15. Wang W, Falk SA, Jittikanont S, Gengaro PE, Edelstein CL, Schrier RW: Protective effect of renal denervation on normotensive endotoxemia-induced acute renal failure in mice. Am J Physiol 283:F583-587, 2003

16. Kaler GM, Truong DM, Khandelwal A, Nagle M, Eraly AS, Swaan PW, Nigam SK: Structural variation governs substrate specificity for organic anion transporter (OAT) homologs. J Biol Chem 282: 23841-23853, 2007

17. Zager RA, Burkhart KM, Johnson AC, Sacks BM: Increased proximal tubular cholesterol content: implications for cell injury and "acquired cytoresistance". Kidney Int 56:1788-1797, 1999

18. Zager RA: Plasma membrane cholesterol: a critical determinant of cellular energetics and tubular resistance to attack. Kidney Int 58:193-205, 2000

19. Banker DE, Mayer SJ, Li HY, Willman CL, Appelbaum FR, Zager RA: Cholesterol synthesis and import contribute to protective cholesterol increments in acute myeloid leukemia cells. Blood. 104:1816-1824, 2004

20. Zager RA, Johnson AC, Hanson SY: Sepsis syndrome stimulates proximal tubule cholesterol synthesis and suppresses the SR-B1 cholesterol transporter. Kidney Int 63:123-33, 2003

21. Kornberg RD: The molecular basis of eukaryotic transcription. Proc Natl Acad Sci USA 104:12955-12961, 2007

22. Li B, Carey M, Workman JL: The role of chromatin during transcription. Cell 128:707-719, 2007

23. Thomas MC, Chiang CM: The general transcription machinery and general cofactors. Crit Rev Biochem Mol Biol 41:105-178, 2006

24. Thewke D, Kramer M, Sinensky MS: Transcriptional homeostatic control of membrane lipid composition. Biochem Biophys Res Commun. 273:1-4, 2000

25. Edwards PA, Tabor D, Kast HR, Venkateswaran A: Regulation of gene expression by SREBP and SCAP. Biochim Biophys Acta. 1529: 103-113, 2000

26. Zager RA, Kalhorn TF: Changes in free and esterified cholesterol: hallmarks of acute renal tubular injury and acquired cytoresistance. Am J Pathol 157:1007-1016, 2000

27. Zager RA, Johnson AC, Hanson SY, Shah VO: Acute tubular injury causes dysregulation of cellular cholesterol transport proteins. Am J Pathol 163: 313-320, 2003

28. Zager RA, Johnson AC, Hanson SY: Parenteral iron therapy exacerbates experimental sepsis. Kidney Int 65:2108-12, 2004

29. Naito M, Bomsztyk K, Zager RA: Endotoxin mediated RNA polymerase II recruitment to target genes in acute renal failure. J Am Soc Nephrol 2008 (in press).

30. Flanagin S, Nelson JD, Castner DG, Denisenko O, Bomsztyk K: Microplate-based chromatin immunoprecipitation method, Matrx ChIP: a platform to study signaling of complex genomic events. Nucleic Acids Res 36: e17, 2008.

FIGURE LEGENDS

Figure 1. Body weight and single kidney weight (as expressed as a percent of total body weight). There was an approximate 3 fold difference in mean body wt for the mice that comprised the three experimental groups. However, single kidney wt remained a relatively constant percent of total body weight.

Figure 2. Severity of ARF for the three age groups, as assessed by BUN concentrations. With each of 3 ARF models, the severity of renal dysfunction increased with advancing age. The p values compare the youngest vs. the oldest groups, whereas the r values reflect the overall correlation coefficients between individual body wts and BUN concentrations for each ARF model (n, 6-10 mice per group). Baseline BUN concentrations were 25±2 mg/dL and did not significantly differ between the groups.

Figure 3. Examples of renal histology obtained from mice in the 'juvenile' vs. the 'mature' mouse groups that were subjected to the maleate (A, B) or glycerol (C, D) model. Maleate treated 'juvenile' mice maintained essentially normal histology (A). Conversely fulminant tubular necrosis with cast formation was observed in the 'mature' group subjected to maleate injection (B). Glycerol had a minimal effect on renal histology in 'juvenile' mice (C). However, glycerol induced marked tubular necrosis and cast formation when administered to 'mature' mice (D).

Figure 4. Effects of increasing maleate and glycerol dosages in 'juvenile' mice on the severity of ARF. Left panel: Increasing maleate from 600 to 800 mg/Kg failed to induce azotemia in 'juvenile' mice. At 1000 mg/Kg, toxicity was apparent, but it was significantly less than that observed in 'mature' mice at a 600 mg/Kg maleate dosage. Right panel: Increasing glycerol dosage from 9 to 12 mg/Kg in 'juvenile' mice induced azotemia, but it was significantly less than that observed in 'mature' mice (n, 5-10 / group).

Figure 5: Renal cortical and serum cholesterol levels in various mouse age groups. As the mice matured from the youngest to the oldest group, a progressive reduction in renal cortical

cholesterol content was observed. Conversely, serum cholesterol levels manifested the opposite trend, since stepwise increases were seen with growth (n, 7-8 per group).

Figure 6: mRNA levels of HMG CoA reductase (HMGCR) and low density lipoprotein receptor (LDL-R) in renal cortex in 'juvenile', 'adolescent', and 'mature' mice. Both HMGCR and LDL-R mRNAs manifested a stepwise decline with age (n, 5-6 per group).

Figure 7. RNA polymerase II (Pol II) density at target gene loci, as assessed by matrix ChIP assay (ref. 30). Pol II was assessed at the start (exon 1) and end exons of the HMGCR and LDL-R genes. The 'juvenile' mice had higher Pol II densities at both HMGCR exons (#1, #19) and both LDL-R exons (#1, #18), compared to the 'mature' mice. These results exactly paralleled the directional changes seen in their cognate mRNAs (n, 6 determinations per group).

Figure 8. Pol II, SREBP-1, and SREBP-2 at the HMGCR promoter region in 'juvenile' and 'mature' mice. Pol II was measured at two sites within the promoter (-100 and -400 base pairs, bp, from 5' to transcription start site, TSS), whereas the SREBPs were measured only at the -100 bp region. The amount of Pol II and both SREBPs were ~2-3x higher in the younger mouse kidneys (n, 6 for each).

Figure 9. 'Negative' controls for Pol II and SREBP recruitment. Left panel: Pol II levels were assessed at ribosomal DNA (rDNA) and there was no difference between the 'juvenile' and 'mature' group. Right panel: The amounts of both SREBPs at a 'silent' (β globin) gene were equal for both mouse groups (n, 6 determinations for each).

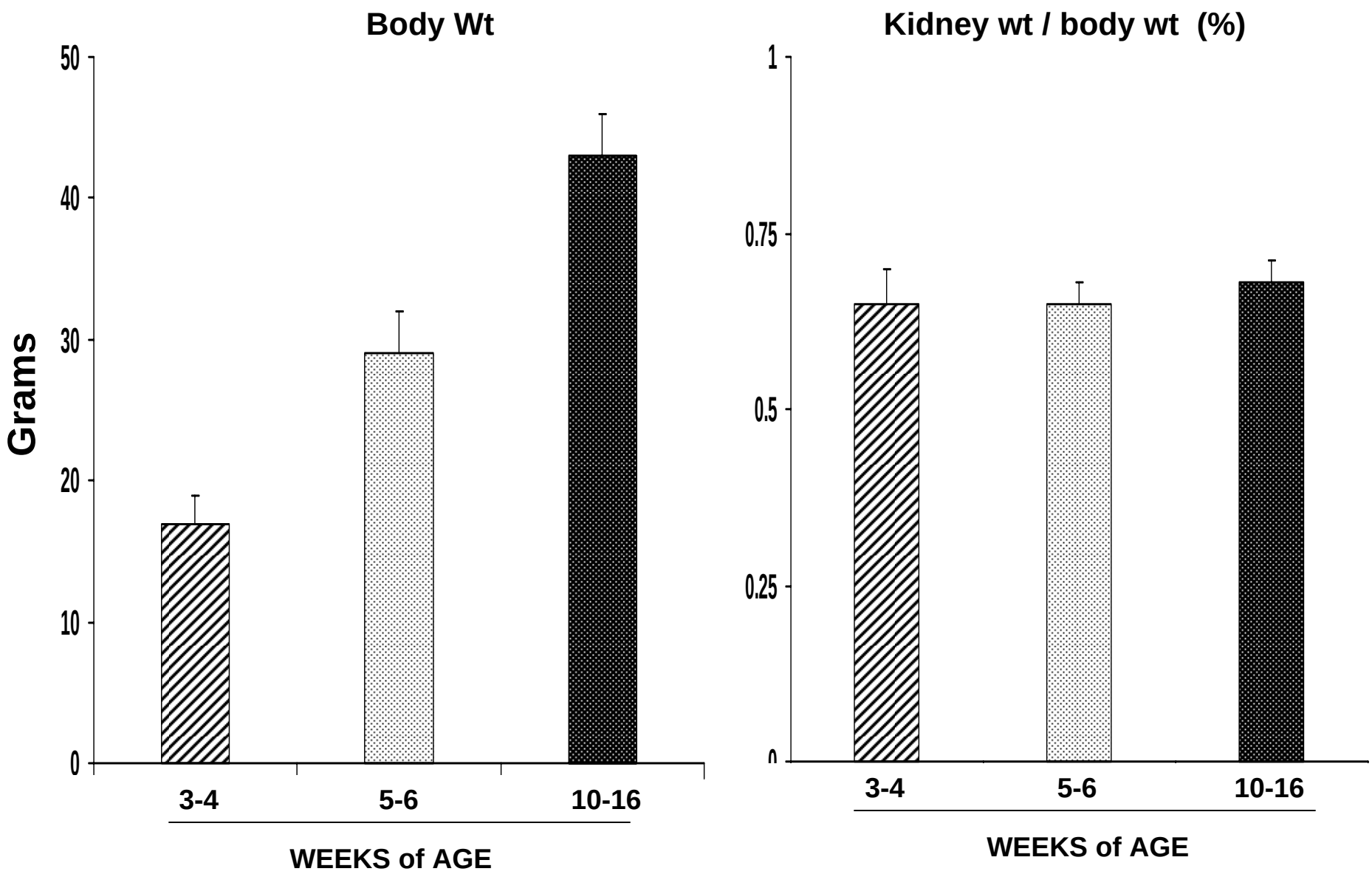
Body Wt
Grams
50
40
30
20
10
0
3-4
5-6
10-16
WEEKS of AGE
Kidney wt / body wt (%)
1
0.75
0.5
0.25
0
3-4
5-6
10-16
WEEKS of AGE

Fig. 1

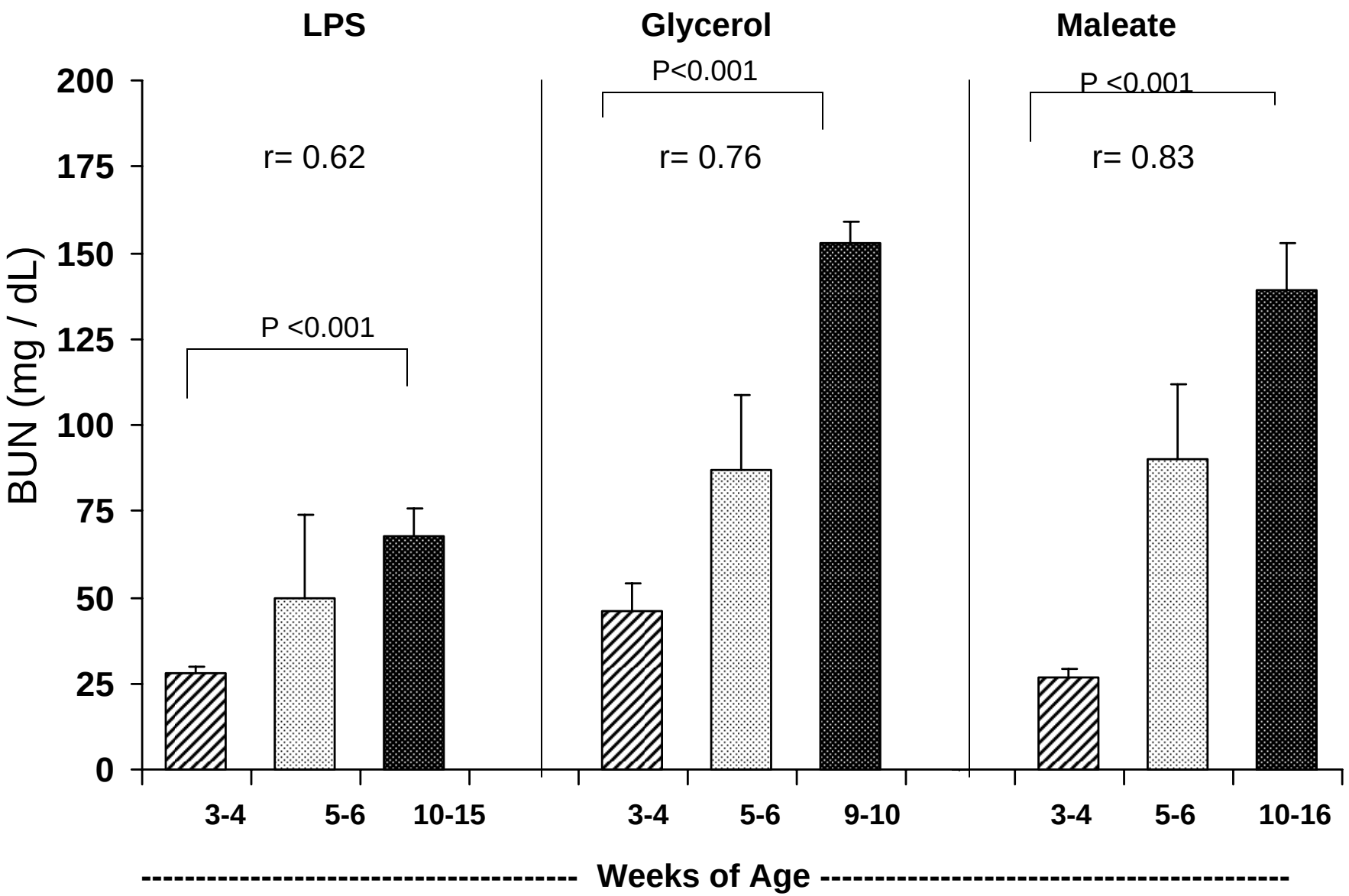
LPS
Glycerol
Maleate
P<0.001
P <0.001
P <0.001
r= 0.62
r= 0.76
r= 0.83
BUN (mg / dL)
200
175
150
125
100
75
50
25
0
3-4
5-6
10-15
3-4
5-6
9-10
3-4
5-6
10-16
Weeks of Age

Fig. 2

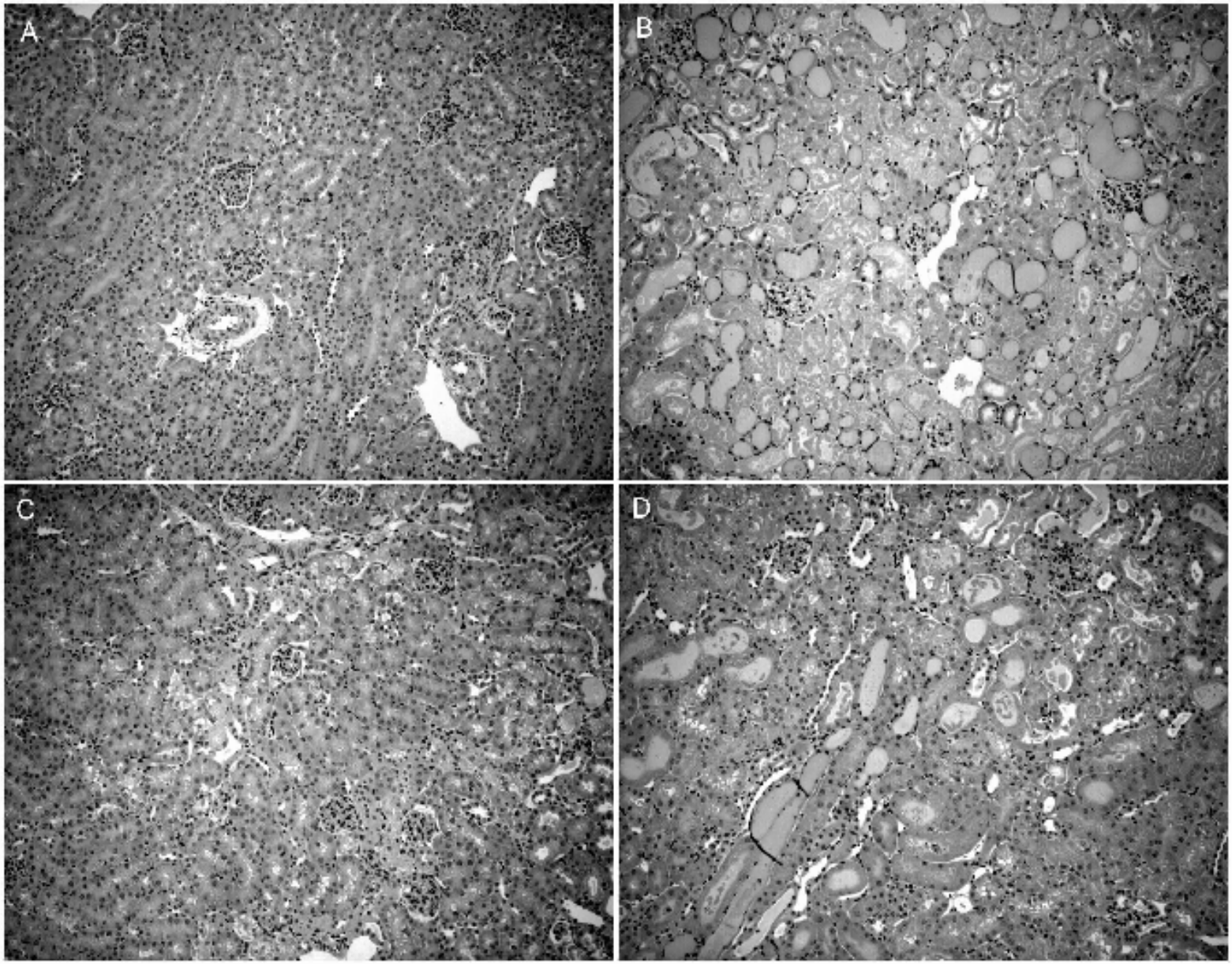

Fig. 3

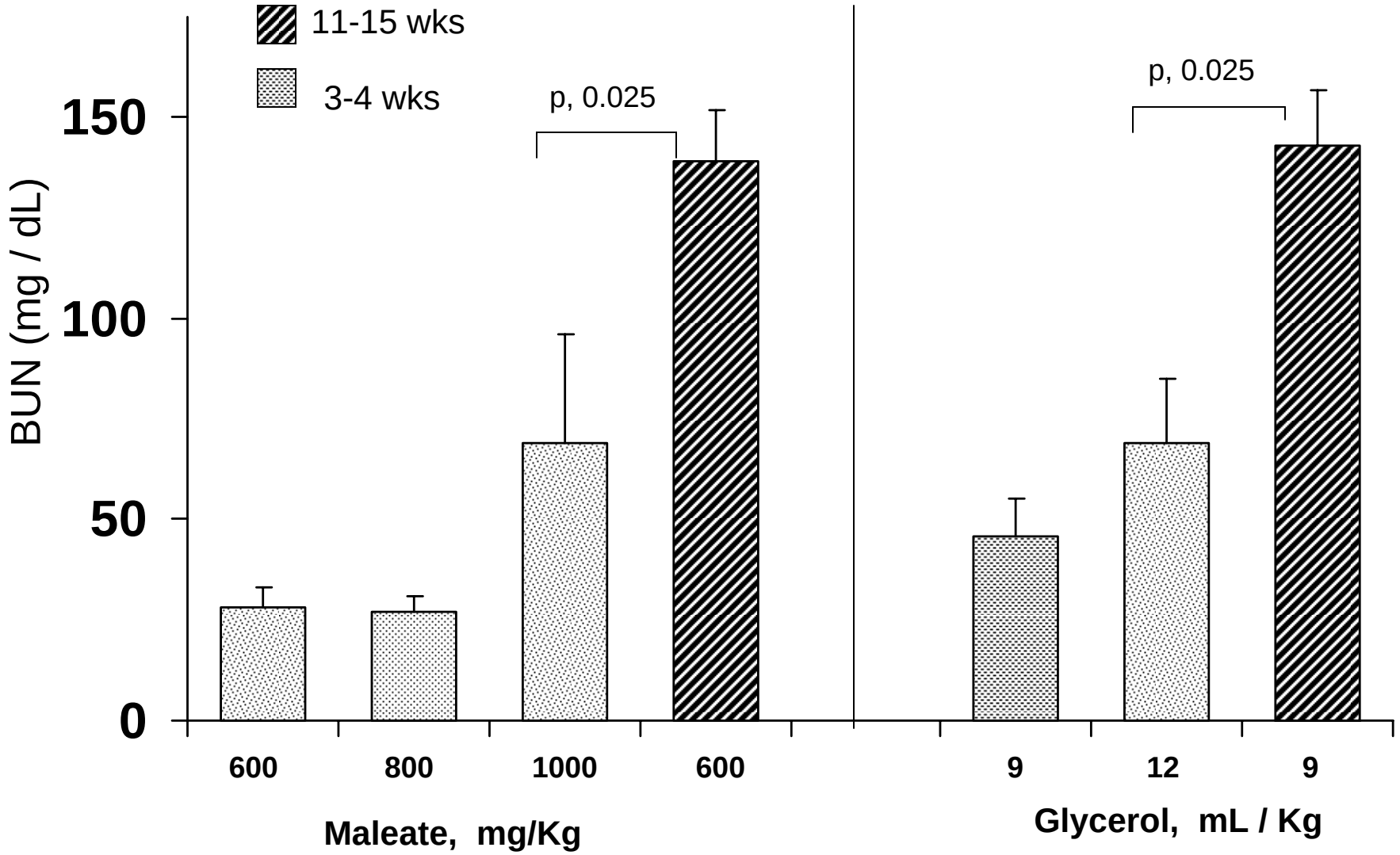
11-15 wks
3-4 wks
p, 0.025
p, 0.025
BUN (mg / dL)
150
100
50
0
600
800
1000
600
9
12
9
Maleate, mg/Kg
Glycerol, mL / Kg

Fig. 4

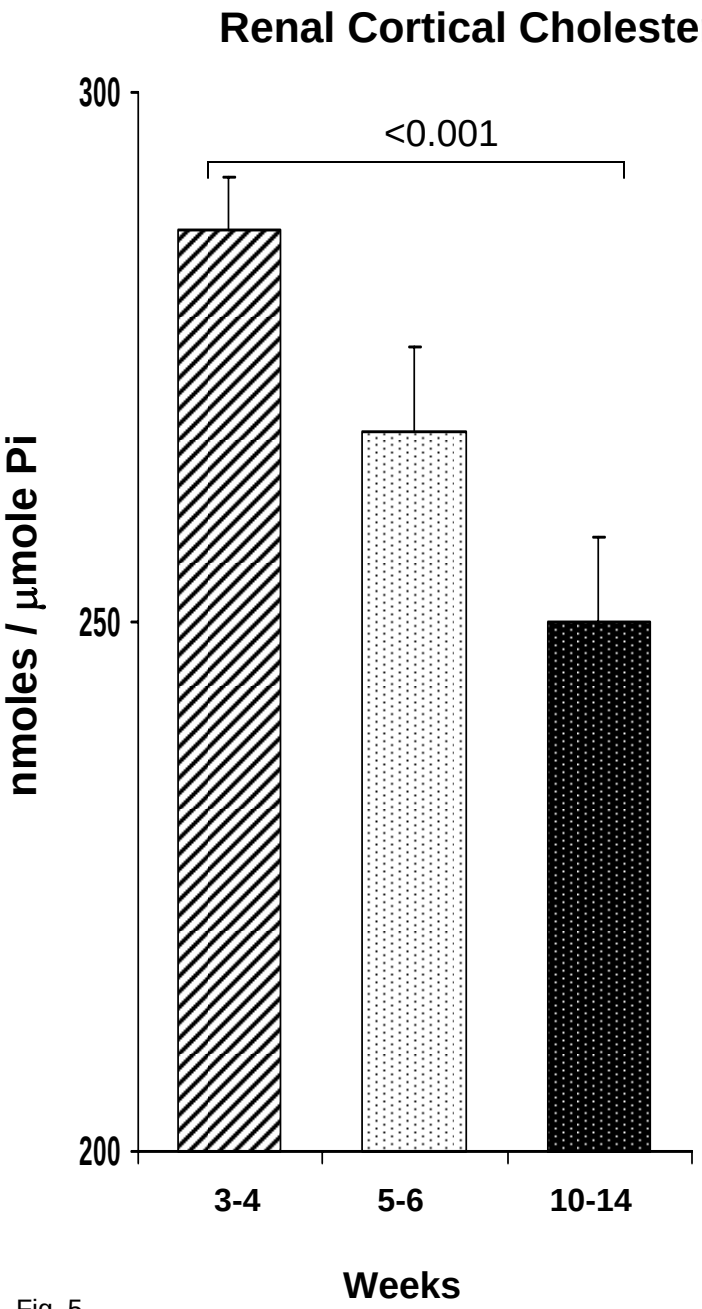
Renal Cortical Cholesterol
300
250
200
nmoles / µmole Pi
<0.001
3-4
5-6
10-14
Weeks

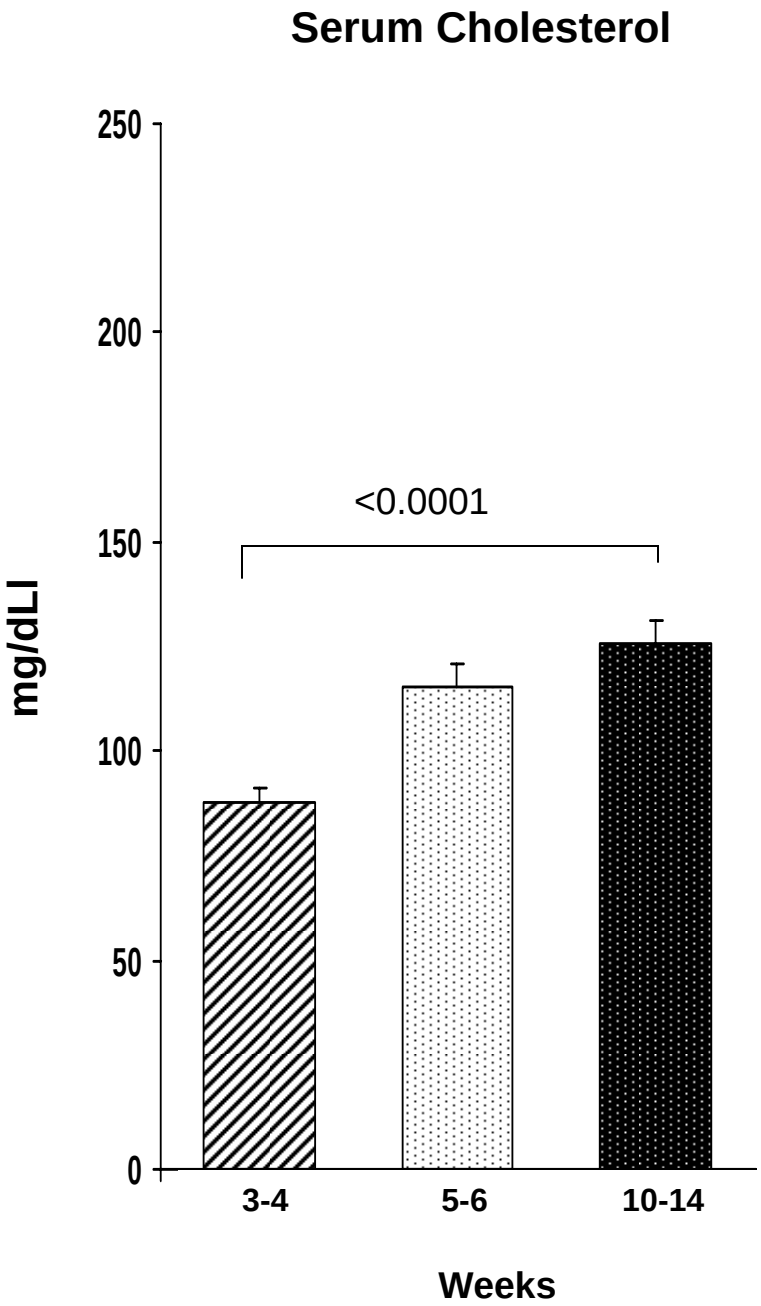
Serum Cholesterol
250
200
150
100
50
0
mg/dLI
<0.0001
3-4
5-6
10-14
Weeks

Fig. 5

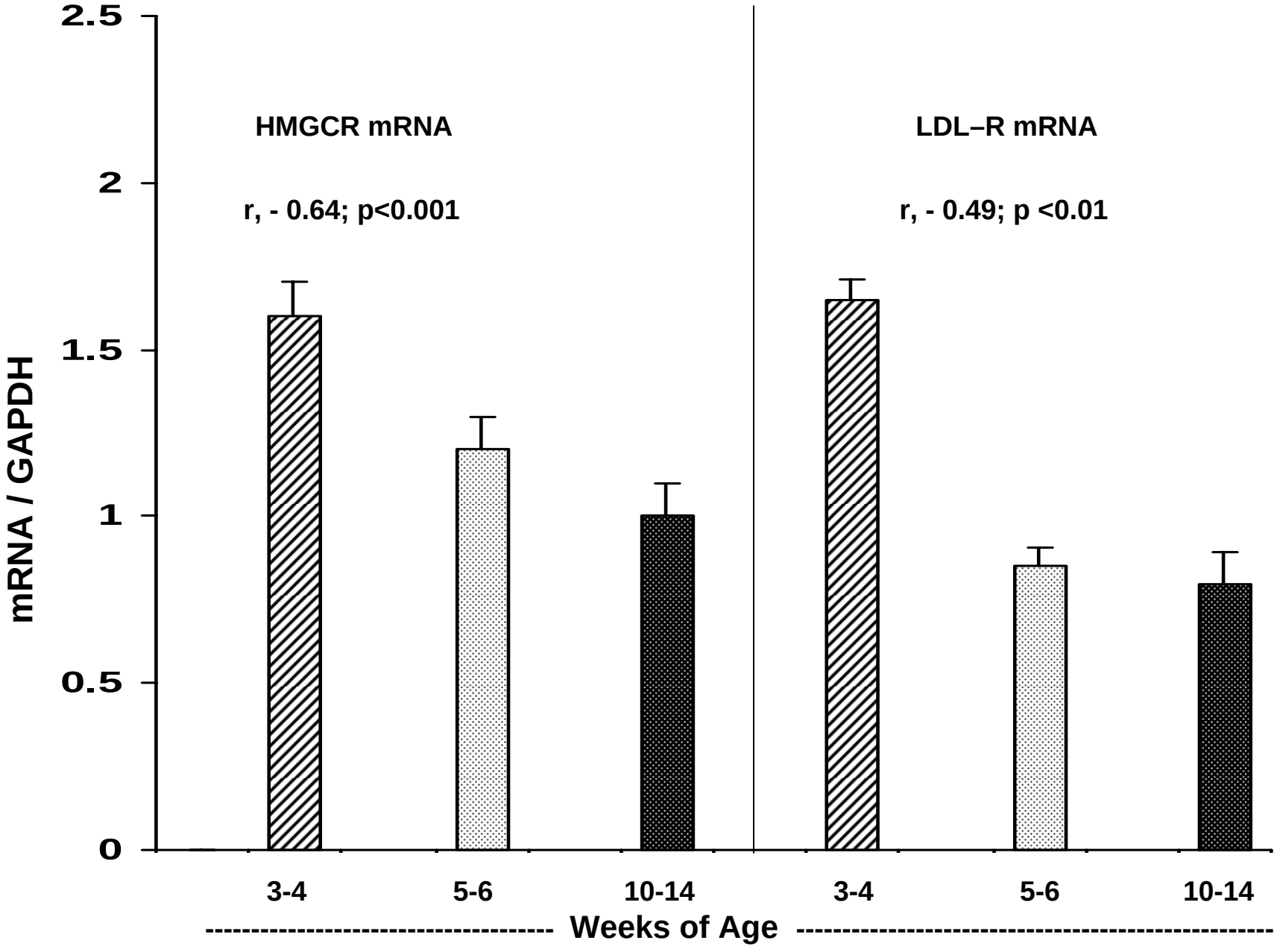
2.5
2
1.5
1
0.5
0
mRNA / GAPDH
HMGCR mRNA
r, - 0.64; p<0.001
LDL–R mRNA
r, - 0.49; p <0.01
3-4
5-6
10-14
3-4
5-6
10-14
Weeks of Age

Fig. 6

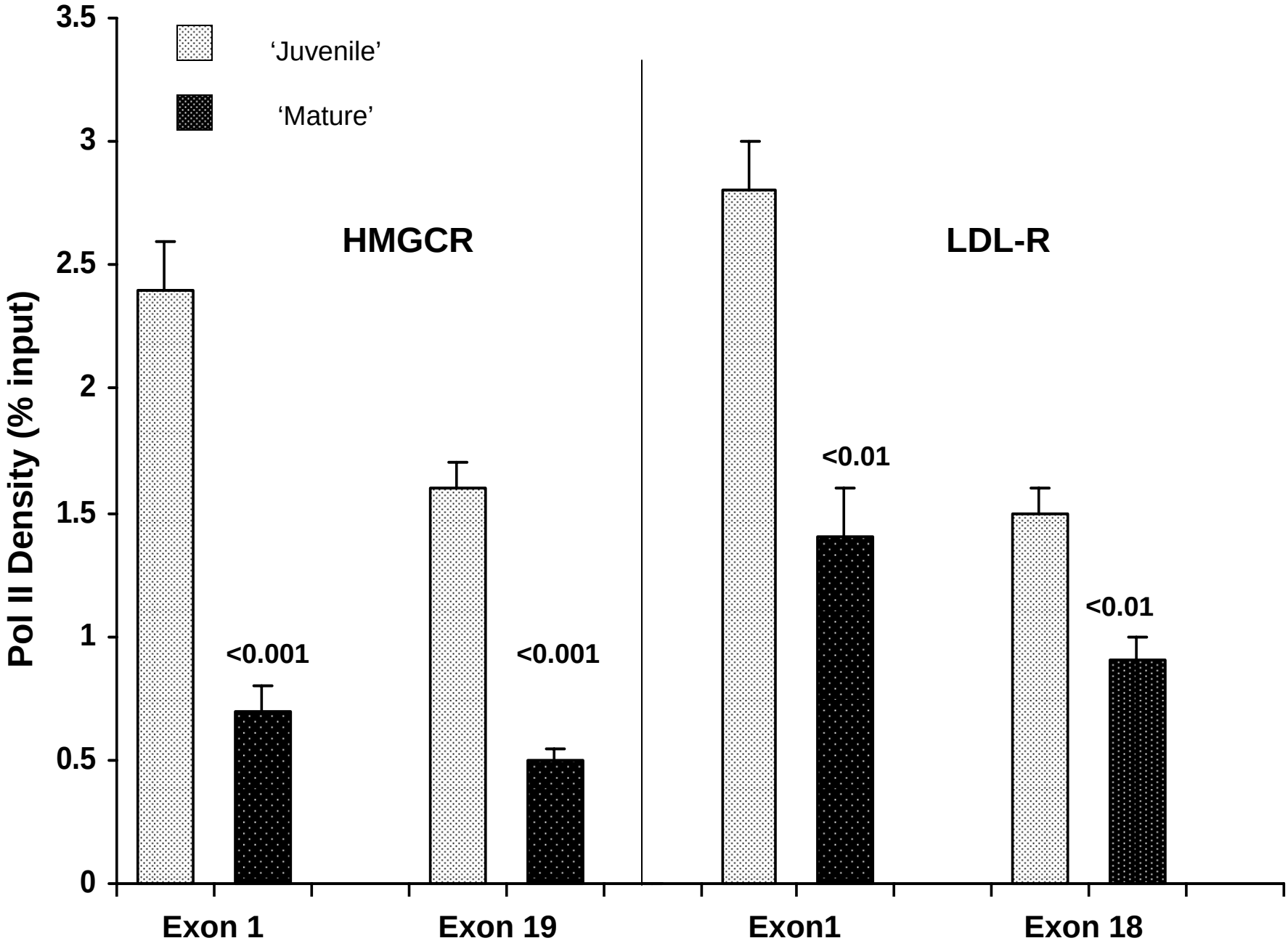
3.5
3
2.5
2
1.5
1
0.5
0
Pol II Density (% input)
'Juvenile'
'Mature'
HMGCR
LDL-R
<0.001
<0.001
<0.01
<0.01
Exon 1
Exon 19
Exon1
Exon 18

Fig. 7

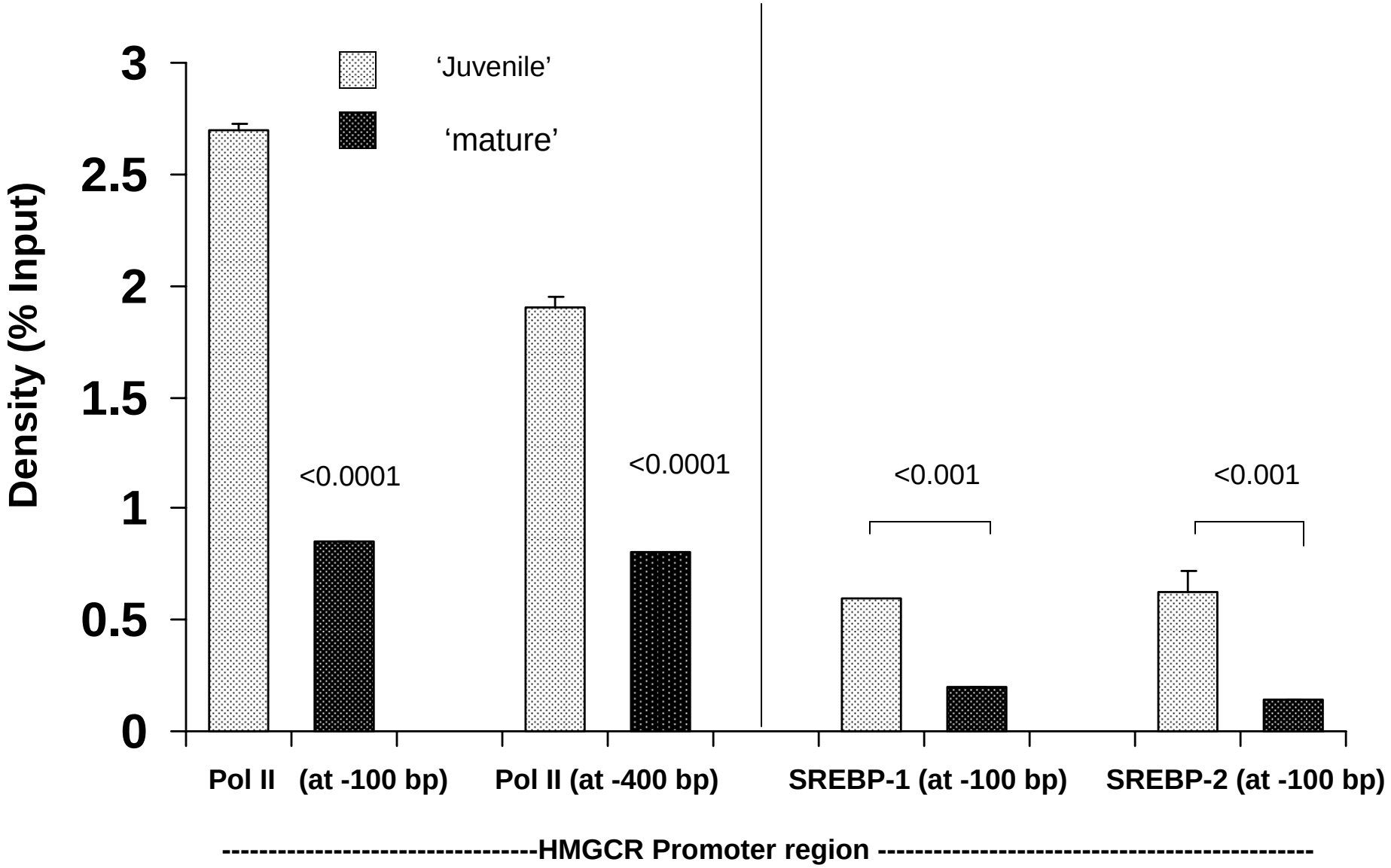
Density (% Input)
3
2.5
2
1.5
1
0.5
0
'Juvenile'
'mature'
<0.0001
<0.0001
<0.001
<0.001
Pol II (at -100 bp)
Pol II (at -400 bp)
SREBP-1 (at -100 bp)
SREBP-2 (at -100 bp)
----------HMGCR Promoter region ----------

Fig. 8

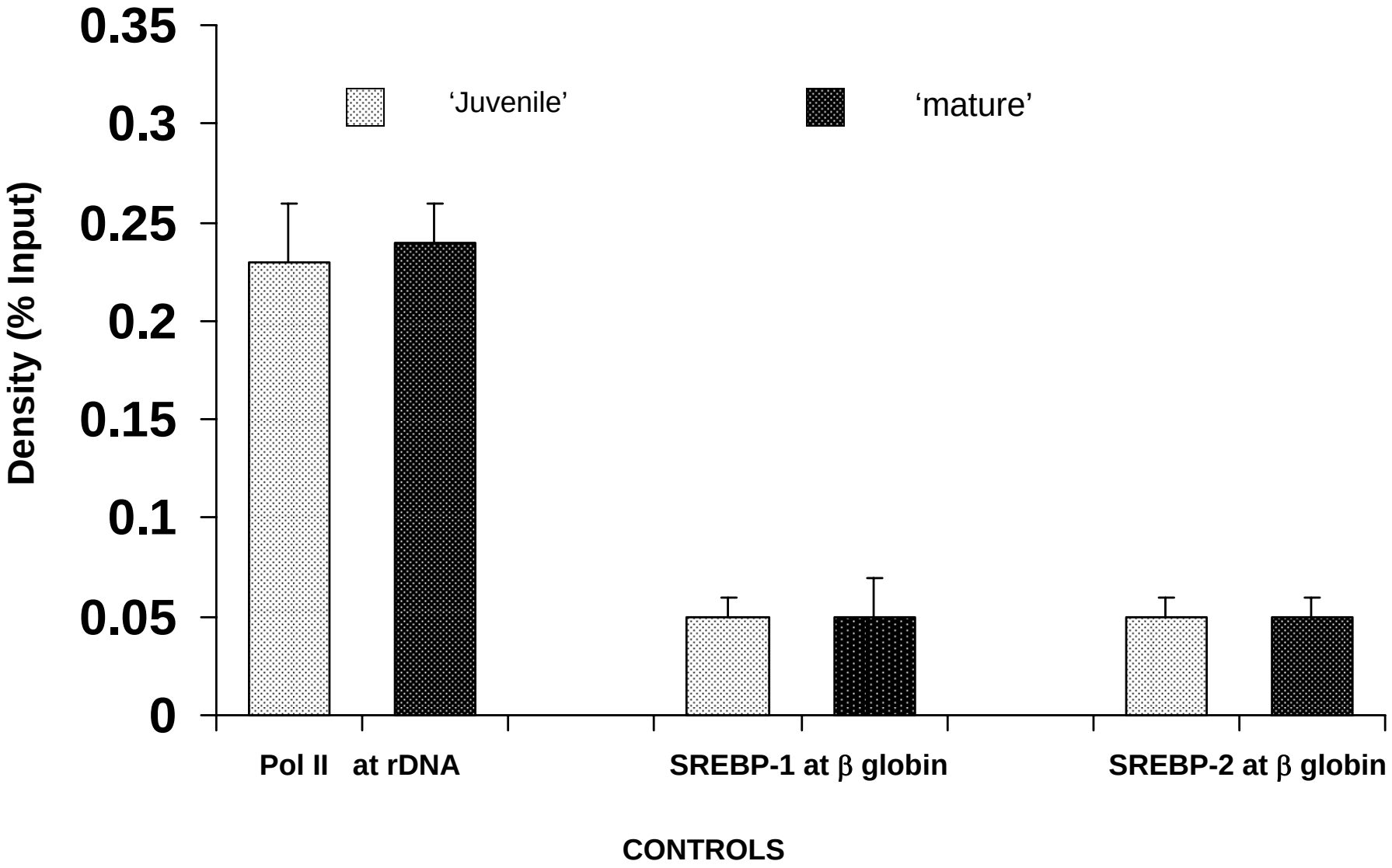
0.35
0.3
0.25
0.2
0.15
0.1
0.05
0
Density (% Input)
'Juvenile'
'mature'
Pol II at rDNA
SREBP-1 at β globin
SREBP-2 at β globin
CONTROLS

Fig. 9